

## MICROLENSING OF CIRCUMSTELLAR DISKS

ZHENG ZHENG<sup>1</sup> AND BRICE MÉNARD

Institute for Advanced Study, Einstein Drive, Princeton, NJ 08540, USA

*Draft version December 2, 2018*

### ABSTRACT

We investigate the microlensing effects on a source star surrounded by a circumstellar disk, as a function of wavelength. The microlensing light curve of the system encodes the geometry and surface brightness profile of the disk. In the mid- and far-infrared, the emission of the system is dominated by the thermal emission from the cold dusty disk. For a system located at the Galactic center, we find typical magnifications to be of order 10-20% or higher, depending on the disk surface brightness profile, and the event lasts over one year. At around 20  $\mu\text{m}$ , where the emission from the star and the disk are comparable, the difference in the emission areas results in a chromatic microlensing event. Finally, in the near-infrared and visible, where the emission of the star dominates, the fraction of star light directly reflected by the disk slightly modifies the light curve of the system which is no longer that of a point source. In each case, the corresponding light curve can be used to probe some of the disk properties. A fraction of  $10^{-3}$  to  $10^{-2}$  optical microlensing events are expected to be associated with circumstellar disk systems. We show that the lensing signal of the disk can be detected with sparse follow-up observations of the next generation space telescopes. While direct imaging studies of circumstellar disks are limited to the solar neighborhood, this microlensing technique can probe very distant disk systems living in various environments and has the potential to reveal a larger diversity of circumstellar disks.

*Subject headings:* gravitational lensing — circumstellar matter

### 1. INTRODUCTION

During the last decade, gravitational microlensing has become a powerful tool for analyzing the distribution and nature of compact dark objects in the halos of our and nearby galaxies. The idea was first suggested by Paczyński (1986) and nowadays a number of monitoring programs are ongoing and have detected several thousands of microlensing event candidates (Alcock et al. 1993, 1996; Aubourg et al. 1993; Udalski et al. 1993, 1994; Udalski 2003; Tisserand & Milsztajn 2005; Afonso et al. 2003a,b; Alcock et al. 2000a,b; Popowski et al. 2003; Calchi Novati et al. 2005). Microlensing can provide us with interesting constraints on the mass of the lenses (e.g., An et al. 2002; Gould et al. 2004; Jiang et al. 2004; Kubas et al. 2005) and the presence of their planetary companions (e.g., Mao & Paczyński 1991; Gould & Loeb 1992; Gaudi et al. 2002; Albrow et al. 2001c; Bond et al. 2004; Abe et al. 2004; Udalski et al. 2005) and circumstellar structures (Bozza & Mancini 2002; Bozza et al. 2002). In addition, several authors have pointed out that microlensing events themselves can yield useful information about the *sources*, i.e., the lensed stars, by taking into account their angular extent (e.g., Gould 1994; Simmons, Newsam, & Willis 1995; Sasselov 1997; Valls-Gabaud 1998; Hendry et al. 1998; Heyrovsky & Loeb 1997; Gaudi & Gould 1999; Cassan et al. 2004; Albrow et al. 2001b; Castro et al. 2001; Gould 2001). For example, the limb-darkening effect of the source star can be used to constrain models of stellar atmosphere, and has been measured in a few microlensing events (e.g., Afonso et al. 2000; Albrow et al. 2000, 2001a; Fields et al. 2003).

In this paper, we discuss another microlensing application: the magnification of a star surrounded by a circumstellar disk. The microlensing properties of such a system appear to be quite interesting: in the optical and near infrared bands, the emission is dominated by the star light and classical Paczyński light curves can be observed, whereas in the mid/far-infrared, the emission from the cold dust of the disk dominates and produces more complex light curves. Microlensing translates spatial structures into temporal ones and allows us to “resolve” the disk. Combining information from both wavelength ranges can place constraints on some of the disk properties. In addition, because of the presence of a disk, a fraction of the star light is reflected by the dusty particles. As this light contribution no longer originates from a point-like source, it will cause the microlensing light curve to slightly deviate from that for star-only in the optical and near-infrared. This effect can also be used to constrain disk properties. Direct imaging studies of disks are possible but are limited, in the foreseeable future, to the vicinity of the solar system. The microlensing technique allows us to access systems that are much further away, i.e., up to  $\sim 10$  kpc. This technique can probe circumstellar disks in various environments with different metallicities and has the potential to reveal the diversity of such systems.

The characteristics of circumstellar disk microlensing light curves differ from those of stars: the total magnification of the disk in the mid-infrared is expected to be significantly smaller than that of a star in the optical. In addition the relative duration of the microlensing event for the disk is expected to be much longer. Indeed, the typical radius of a circumstellar disk  $a$  is of the order of a few tens of AU, though it depends on the age and type of the central star (Zuckerman 2001). For a source at the

<sup>1</sup> Hubble Fellow

Galactic center and a lens of  $1 M_{\odot}$  located halfway, the Einstein ring radius  $\hat{r}_E$  in the source plane is about 8AU, which is much smaller than the source (disk) size. We therefore have an extreme finite source effect and only that part of the source inside the Einstein ring is efficiently magnified. For a large uniform face-on disk, the expected overall fractional flux excess caused by the lensing effect is  $2(\hat{r}_E/a)^2$  (Agol 2003), which is at the level of  $\sim 10\%$  if the disk radius is a few times larger than  $\hat{r}_E$ . The microlensing timescales are also different. For a star, the duration of the lensing event  $t_E$ , i.e., the time required to cross the Einstein radius, is about one month. For a circumstellar disk, this timescale is about  $(a/\hat{r}_E)t_E$ , which ranges between half a year to a couple of years. If a microlensing event of a (young) star is discovered (in optical or infrared), one can then (sparsely) monitor the object in the mid-infrared and look for the excess characteristic of circumstellar disks. If a disk can be detected, then observing its flux as a function of time will provide us with constraints on the disk size and brightness distribution as the lens differentially resolves the disk.

In this paper we show that next generation space telescopes will be able to detect microlensing events of circumstellar disks at the Galactic center. The outline of this paper is as follows. In § 2, we present some characteristic parameters of circumstellar disks. In § 3, we introduce the formalism describing the observed light curve of a disk. In § 4, we show how the disk parameters are related to the shape of the light curve and the behaviors of light curves in different observational bands. We then investigate the detectability and the occurrence of this phenomenon in § 5. Finally, we summarize and discuss our results in § 6.

## 2. CHARACTERISTICS OF CIRCUMSTELLAR DISKS

Circumstellar disks evolve through two main stages: during the first phase, the protoplanetary disk composed of gas and dust is optically thick and provides a particle reservoir for planet formation. By the time stars of  $\sim 1 M_{\odot}$  reach ages of  $\sim 1$  Myr, the accretion disk surrounding the stars has lost its gas, becomes optically thin and readily accessible to observation at many wavelengths. It is referred to as a debris disk. The dust particles in the disk absorb a fraction of the star's photons and re-emit them at longer wavelengths. The parameters of some debris disks observed in the vicinity of the solar system are listed in Zuckerman & Song (2004). Current observations show that typical systems have a star temperature of about 6000 K and the excess infrared emission from the disk can be well fitted by a blackbody spectrum with an effective temperature of about 80 K. This does not imply that the disk is isothermal but is simply a useful way for describing the disk spectral energy distribution.

Apart from the re-emitted light, some of the star photons intercepted by the disk are reflected. The relative amount of light being reflected and that being absorbed and re-emitted depends on the albedo of the disk, which is of the order of a few tens of percent. For simplicity, we assume the albedo to be 0.5 so that the disk seen through the reflected light and through the re-emitted light has the same luminosity, which we denote as a fraction  $\tau$  of the star's bolometric luminosity.

It has been empirically found that the fraction  $\tau$  de-

pends on the age of the system,  $\tau \propto \text{age}^{-1.75}$  for ages between  $10^{6.5}$  and  $10^{9.5}$  years (Zuckerman & Song 2004). For a 10 Myr system and a 100 Myr system,  $\tau \sim 10^{-2}$  and  $\sim 2 \times 10^{-4}$ , respectively. The expected spectral energy distribution of such systems located at the Galactic center (a distance of  $D = 8$  kpc), is illustrated in Figure 1 for different values of  $\tau$ . In this plot we have not considered extinction effects as they are in general small for the wavelength ranges we consider below. As can be seen, the infrared excess caused by the thermal emission of the disk decreases rapidly as the system ages. In the figure we have assumed that the reflected light from the disk has the same spectral energy distribution as the star.

Circumstellar disks are expected to have an inner disk radius set by the sublimation temperature of the dust grain (Natta et al. 2001) with radii ranging from around one to a few AU, and in addition, theoretical models predict that planets in disks can interact with the disk material and open wide radial gaps (Papaloizou & Lin 1984; Paardekooper & Mellema 2004), once they achieve sufficient mass. The width of the gap is expected to be  $\sim 20\%$  of the orbital radius, which would decrease the disk surface density in a 1 AU annulus at 5 AU for example. In addition disk structures such as rings, warps and blobs are expected as a result of the presence of planets (Moran et al. 2004; Kuchner & Holman 2003; Wilner et al. 2002; Wyatt & Dent 2002; Quillen & Thorndike 2002; Wahhaj et al. 2003; Koerner et al. 2001) and will be imprinted in the microlensing light curve of the system and, in some cases, might enhance the detectability of the disk.

At the Galactic center, the angular size of a 30 AU disk is only  $\sim 0.004''$ . Spatially resolving such system in the visible and mid-infrared would require a telescope larger than 30 m, and 1 km respectively. With microlensing, however, the spatial information is translated into a temporal one. As shown below, measuring the microlensing light curve allows us to probe the disk geometry and surface brightness profile.

## 3. THE FORMALISM OF MICROLENSING OF DISKS

The characteristic scale for microlensing is the Einstein radius of the lens. For our purpose in this paper, the Einstein radius is defined in the *source* plane, which reads

$$\begin{aligned} \hat{r}_E &= \left[ \frac{4GM}{c^2} \frac{(D_s - D_l)D_s}{D_l} \right]^{1/2} \\ &= 8.1 \text{ AU} \left( \frac{M}{M_{\odot}} \right)^{1/2} \left( \frac{D_s}{8 \text{ kpc}} \right)^{1/2} \left( \frac{1-x}{x} \right)^{1/2}, \end{aligned} \quad (1)$$

where  $M$  is the lens mass,  $x = D_l/D_s$ , and  $D_s$  and  $D_l$  are the distances to the source and lens, respectively. For a source at the Galactic center and a  $1 M_{\odot}$  lens located half way,  $x = 1/2$  and  $\hat{r}_E \simeq 8$  AU. The corresponding time scale for the source to cross the Einstein radius is

$$\begin{aligned} t_E &= \hat{r}_E/v \\ &\simeq 70 \text{ days} \left( \frac{M}{M_{\odot}} \right)^{1/2} \left( \frac{D_s}{8 \text{ kpc}} \right)^{1/2} \\ &\quad \times \left( \frac{1-x}{x} \right)^{1/2} \left( \frac{v}{200 \text{ km/s}} \right)^{-1}, \end{aligned} \quad (2)$$

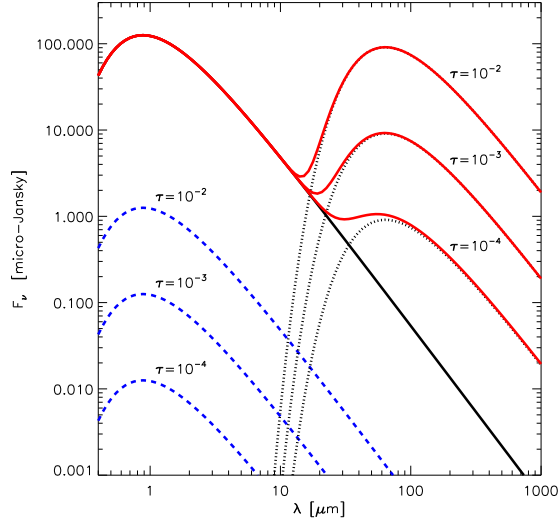


FIG. 1.— Spectral energy distribution of a star with  $T = 5800K$  surrounded by a dusty debris disk with  $T = 80K$ . This system is put at the Galactic center (distance  $D = 8$  kpc). The reflected (dashed curves) and re-emitted (dotted curves) lights from the disk are calculated for three values of the disk-to-star luminosity ratio:  $\tau = 10^{-2}$ ,  $10^{-3}$ , and  $10^{-4}$ .

where  $v = D_s \mu_{\text{rel}}$  and  $\mu_{\text{rel}}$  is the relative proper motion between the source and the lens.

Considering the central star as a point source, the magnification  $A$  of the source can be shown to depend only on the projected separation  $u$  of the lens and source, in units of  $\hat{r}_E$  of the lens (Paczynski 1986), namely

$$A(u) = \frac{u^2 + 2}{u \sqrt{u^2 + 4}}. \quad (3)$$

The relative motion between the source and the lens changes  $u$  and therefore the magnification varies as a function of time. Microlensing events of point sources can be identified from this characteristic light curve.

Heyrovsky & Loeb (1997) considered the microlensing of inclined accretion disks of active galactic nuclei. In this case, the Einstein ring radius is much larger than the size of the source and large magnification values can be reached. The case considered in this paper is different: the size of Galactic circumstellar disks is larger than the Einstein ring radius leading to lower magnifications and longer timescales. For the magnification of very large sources, a number of analytical approximations have been derived in the literature (Heyrovsky & Loeb 1997, Agol 2003). In our case, the Einstein ring is not necessarily much smaller than the spatial extents of features in the disk, therefore we proceed with the exact calculations.

In this paper we do not intend to model the disk in great details. For estimating the lensing signal we will use different surface brightness profiles in order to represent the changes in dust and temperature distributions. Let us now consider an axially symmetric disk with surface brightness profile  $f(a)$ , where  $a$  is the radial distance to the central star. The projection of the disk onto the sky plane is an ellipse. The configuration of the disk is fixed given its center position  $(R, \Phi)$  with respect to the lens, the inclination angle  $i$ , and the orientation angle  $\phi_0$

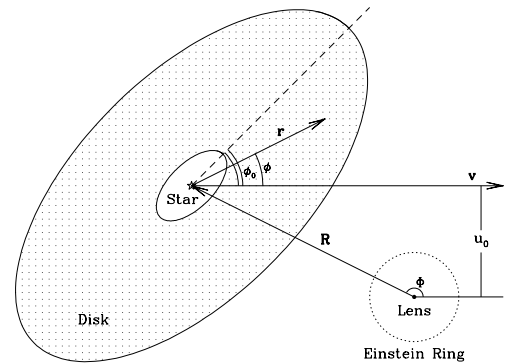


FIG. 2.— Geometry of lensing of a circumstellar disk. The dotted ring around the lens indicates the Einstein ring. The circumstellar disk is assumed to have a hole inside an inner radius and a cutoff outside an outer radius. Projected onto the sky plane, the disk appears to be an ellipse with the orientation angle of the major axis being  $\phi_0$ . Any point on the disk is specified by its coordinates  $(r, \phi)$  in a polar system centered at the star. The angles  $\phi_0$  and  $\phi$  are with respect to the direction of the relative motion  $\mathbf{v}$ . The position of the star (or the disk center) is specified by  $(R, \Phi)$  with respect to the lens ( $\Phi$  is relative to the direction of  $\mathbf{v}$ ). The impact parameter of the star is denoted as  $u_0$ .

of the projected major axis (with respect to the direction of the relative motion). The geometry and meanings of symbols are shown in Figure 2. In all our discussions below, quantities with length dimension are in units of the Einstein ring radius  $\hat{r}_E$  and surface brightnesses are in units of  $\text{flux}/\hat{r}_E^2$ . We consider a geometrically thin disk with isotropic emission at every point. With no lensing effect, the total flux of the disk can be calculated without projection and is given by

$$F_0 = \int \int f(a) a da d\phi = 2\pi \int f(a) a da. \quad (4)$$

If the disk is lensed, the total flux is the unlensed flux convolved with the magnification profile  $A(u)$ ,

$$F = \int \int A(u) f_p(r, \phi) r dr d\phi, \quad (5)$$

where  $f_p$  is the projected surface brightness profile,  $u = [R^2 + 2Rr \cos(\Phi - \phi) + r^2]^{1/2}$  is the distance from the lens to a (projected) disk element. Here  $(r, \phi)$  are polar coordinates with origin at the center of the star (see Figure 2). The integration becomes easier if we change the variable  $r$  to the radius  $a$  along the major axis according to the relation  $a = r \sqrt{1 + \sin^2(\phi - \phi_0) \tan^2 i}$ . The projected surface brightness  $f_p$  is simply  $f(a)/\cos i$ . Equation (5) then has the form

$$F = \int \int A(u) \frac{f(a)}{\cos i} \frac{a}{1 + \sin^2(\phi - \phi_0) \tan^2 i} da d\phi. \quad (6)$$

The overall magnification of the disk flux is  $F/F_0$ . The temporal dependence of the magnification is through the

position of the disk center  $(R, \Phi)$  with respect to the lens,

$$R(t) = \sqrt{t^2 + u_0^2} \quad \text{and} \quad \Phi(t) = \arccos \frac{t}{\sqrt{t^2 + u_0^2}}, \quad (7)$$

where  $u_0$  is the impact parameter in unit of  $\hat{r}_E$ , and  $t$  is the time in unit of  $t_E = \hat{r}_E/v$  defined in equation (2). We set  $t = 0$  at  $\Phi = \pi/2$ .

From equation (6), we see that the light curve of the disk depends on the magnification kernel  $A(u)$  and the geometry and the surface brightness profile of the disk. It should be noted that  $A(u)$  can be directly inferred from observations of the light curve of the star in optical or near-infrared band. The disk light curve can be used to constrain  $f(a)$  and the geometric parameters only.

Before investigating the expected light curves described by the exact results of equation (6), it is interesting to get a more intuitive understanding of this equation by considering the following approximation: if the spatial features of the disk are much larger than the Einstein ring radius, the calculation of the magnification can be simplified by approximating  $A(\mathbf{u}) - 1$  as  $2\pi\delta_D(\mathbf{u})$ , where  $\delta_D$  is the Dirac- $\delta$  function. The increase in flux  $\Delta F = F - F_0$  caused by the lensing simply traces the local surface brightness of the disk at the position of the lens (i.e.,  $\mathbf{r} = -\mathbf{R}$ ). The result is

$$\Delta F = 2\pi f_p(r, \phi) = 2\pi f(a) / \cos i, \quad (8)$$

where  $r = R(t)$ ,  $\phi = \Phi(t) - \pi$ , and  $a$  is related to  $r$  and  $\phi$  as mentioned above equation (6). The excess flux is just twice the Einstein ring area times the surface brightness at the lens position, which is the same as derived by Heyrovsky & Loeb (1997) (see their eq.[34]) for an elliptical source and by Agol (2003) (see his eq.[10]) for general large sources. In fact, the result of the magnification for a large source presented in Agol (2003) (his eq.[4]) can be derived as above by noticing that  $A(\mathbf{u}) - 1 \simeq 2\pi\delta_D(\mathbf{u})$ . Approximate calculations of the magnification at the edge of a large source can be found in Agol (2003).

It should be noted that the light curve alone is not sufficient to determine the physical size of a disk and what we infer are all in units of the Einstein ring radius. Additional information on the size of the Einstein ring radius could be obtained from the star-only light curve if the finite source effect and the parallax effect are detected. The former gives the angular size of the Einstein ring radius with respect to that of the source star (e.g., Gould 1994) and the latter measures the Einstein ring radius projected onto the observer's plane (see, e.g., Gould 1992; Jiang et al. 2004; Gould et al. 2004). Since the impact parameter needs to be small for a measurable finite source effect, it is unlikely that the lensing of a system with circumstellar disk can measure the angular size of the Einstein ring. Even if we have both the relative angular size of the Einstein ring and its projected size onto the observer's plane, we still need the source distance in order to infer the size of the Einstein ring projected onto the *source* plane. The radial velocity of the source star could provide some information on the source distance. If the blended light in the microlensing event is caused by the lens, which can be verified astrometrically, information about the mass and distance of the lens can be obtained (Ghosh et al. 2004). Finally, if we observe the event at different wavelengths, the temperature as

a function of radius in units of the Einstein ring radius can be constrained. Then, by knowing the dust particle albedo, measuring the central star temperature, and assuming thermal equilibrium, the corresponding physical radii can be inferred. In general, we may have to rely on some statistical priors to constrain the physical size of the disk.

#### 4. OBSERVATIONAL SIGNATURES

##### 4.1. Mid- and Far-infrared: Re-emitted Light

In the mid- and far-infrared, the luminosity of the system is dominated by the light re-emitted by the disk and the contribution of the star can be neglected. The light curve of the disk depends on its geometrical properties (the size, the inclination angle  $i$ , the orientation angle  $\phi_0$  of the projected major axis, and the impact parameter  $u_0$ ) and its surface brightness profile. To show its dependence on various parameters, we assume that the disk has an inner radius  $a_i$  and an outer radius  $a_o$  with a power-law surface brightness profile  $f(a) \propto a^\alpha$  between these two radii. The light curves are shown in Figure 3 with  $a_i$ ,  $a_o$ ,  $i$ ,  $\phi_0$ ,  $u_0$ , and  $\alpha$  varied, one at a time.

As shown in panel (a), the existence of an inner radius of the disk causes a corresponding dent in the light curve because the disk is less efficiently magnified as the lens comes close to the inner radius. The dent becomes deeper as the inner radius becomes larger. The width of the dent is proportional to the inner radius. Similarly, radial gaps opened by planets in the disk will also exhibit such dents in the light curve. Panel (b) shows cases for which the outer radius varies: the smaller the disk, the larger the magnification as the percentage that can be effectively lensed becomes larger. The overall magnification is inversely proportional to  $a_o^2 - a_i^2 \sim a_o^2$ , and the duration time is proportional to  $a_o$ .

The area of the disk projected onto the sky plane depends on the inclination angle, i.e., proportional to  $\cos i$ . With other parameters fixed, a more inclined disk would have a higher overall magnification, as shown in panel (c), because its projected area is smaller and it becomes more efficiently magnified. On the other hand, the orientation of the projected disk does not change the area, and has therefore little effect on the maximum magnification. This is shown in panel (d). However, the duration has a dependence on the orientation, since it changes the path length that the lens crosses the disk. Except for cases with  $\phi_0 = 0^\circ$  and  $90^\circ$ , the orientation of the disk (plus the non-zero impact parameter) also causes the light curve to be asymmetric about  $t=0$ .

In panel (e), we investigate the effect of the surface brightness profile of the disk. With a more concentrated surface brightness profile, the disk appears to be less extended, and the maximum magnification increases. In our example, the maximum amplitude changes from  $\sim 15\%$  for a uniform disk to  $\sim 40\%$  for a disk with surface brightness  $\propto a^{-2}$ . Slopes at the rising and fading parts of the light curve also probe the surface brightness profile, in the sense that a steeper light curve corresponds to a steeper brightness profile. As we mention in § 3, if the disk is much larger than the Einstein ring, the light curve simply traces the surface brightness profile along the lens trajectory.

For a point source, the magnification is determined by the impact parameter  $u_0$ . However, for a disk close to

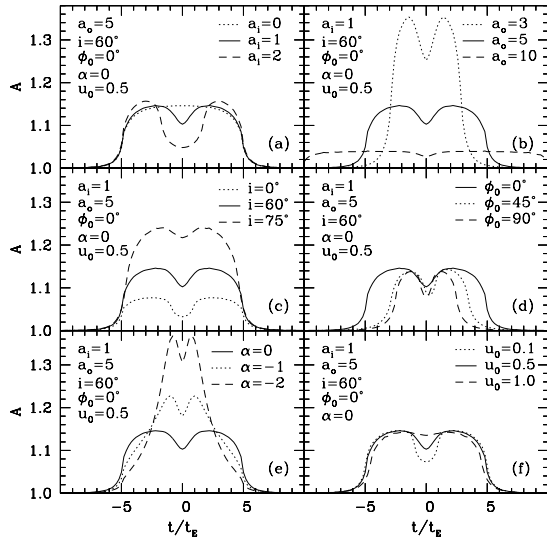


FIG. 3.— Lensing light curves of the disk. In each panel, one disk parameter is varied as indicates at the upper-right corner with others fixed at values listed at the upper-left corner. The y-axis is the magnification. The disk parameters include the inner radius  $a_i$ , the outer radius  $a_o$ , the inclination angle  $i$ , the orientation angle  $\phi_0$  of the projected major axis, the surface brightness profile index  $\alpha$ , and the impact parameter  $u_0$ . Parameters with length dimension are in units of the Einstein ring radius.

uniform, the impact parameter has little effect on the magnification of the disk flux, since the magnification is largely determined by the area ratio of the Einstein ring to the projected disk. Panel (f) shows that, because of the inner hole in the disk, a smaller impact parameter leads to a deeper dent in the light curve.

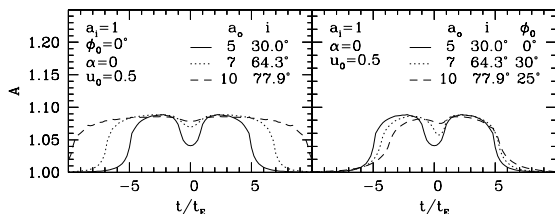


FIG. 4.— Lensing light curves with similar magnification. In the left panel, values of the outer radius  $a_o$  and the inclination angle  $i$  are changed in a way to keep the projected area of the disk fixed  $[(a_o^2 - a_i^2) \cos i = \text{constant}]$ . In the right panel, additional changes of the orientation angle  $\phi_0$  are made to match the duration time.

After having seen how the light curve responds to different parameter changes, it should be noted that a number of parameter combinations could be degenerate. To first order, the light curve of a uniform disk can be characterized by the maximum magnification and the duration time. As we have discussed, the magnification is largely determined by the area ratio of the Einstein ring to the projected disk. For example, a larger disk that is highly inclined could have the same projected area as a smaller disk that is slightly inclined. The magnifications for the two cases would be similar. The degenerate direction of the magnification roughly follows  $(a_o^2 - a_i^2) \cos i = \text{constant}$ . The left panel of Figure 4

shows examples with  $(a_o^2 - a_i^2) \cos i$  fixed. As expected, the amplitudes of the light curves are similar. The duration time (in unit of  $t_E$ ) of the event is the length (in unit of  $\hat{r}_E$ ) of the chord the lens crosses. For a larger disk, it becomes longer, but this can change if we vary the orientation of the projected disk as seen in panel (d) of Figure 3. By adjusting the orientation parameter  $\phi_0$ , we can have light curves that mimic each other, as shown in the right panel of Figure 4. The asymmetry of the light curves can break the degeneracy. But if the data are noisy, the solution would be partially degenerate with respect to the size of the disk, the inclination angle, and the orientation angle.

The above degeneracy can be broken by making use of the star-only light curve (in optical or near-infrared band). The orientation of the disk leads to a difference in the time of the center of the disk-only event with respect to the star-only event. This time difference, together with the impact parameter inferred from the star-only light curve, gives the orientation. Once the orientation is known, the duration time, which corresponds to the chord length, and the magnification, which is related to the area of the projected disk, can be used to infer the size and the inclination of the disk. For a realistic, non-uniform disk, the surface brightness profile has the effect to make the light curve more asymmetric if the orientation is neither  $0^\circ$  nor  $90^\circ$ . This also helps to break the degeneracy between the orientation and the inclination (with the assumption of a circular, azimuthally symmetric disk in projection).

#### 4.2. The $\sim 20\mu\text{m}$ Transition

For a large range of disk-to-star luminosity ratios and temperatures, the flux of the star becomes as important as that of the disk in the  $\sim 10 - 20\mu\text{m}$  wavelength range. As a point source, the star has its flux highly magnified, while the amplification of the disk flux is, as seen above, at the 10-20% level and lasts over a longer period. An interesting phenomenon in this case is that the lensing event appears to be chromatic if we compare the light curve in optical and that at  $\sim 20\mu\text{m}$ . The reason is as follows: in optical, the baseline flux (unlensed flux) is from the star and the whole flux is magnified by the lens. At  $\sim 20\mu\text{m}$ , the baseline flux is the sum of those from the star and the disk, but only the star's flux is highly magnified by the lens. Therefore, the apparent magnification of the star+disk system is much less than that for the star. That is, if the fraction of the unlensed fluxes from the star and the disk are  $x$  and  $1 - x$ , the magnification of the system is then  $x A_\star + (1 - x) A_d$ , where the magnification  $A_\star$  of the star is much larger than  $A_d$ , that of the disk. Figure 5 shows an example of the light curve for the system in optical and at  $\sim 20\mu\text{m}$  with the assumption that the star and the disk have the same flux ( $x = 0.5$ ) at  $\sim 20\mu\text{m}$ . The apparent chromatic effect can happen if the system to be lensed has different spatial structures in two bands or there is a color gradient across the (large) system.

#### 4.3. Visible and Near-infrared: Reflected Light

It is interesting to note that constraints on the disk can also be obtained at shorter wavelengths where the star flux largely dominates: a fraction  $\tau$  of the star light is directly reflected by the circumstellar dust (so strictly

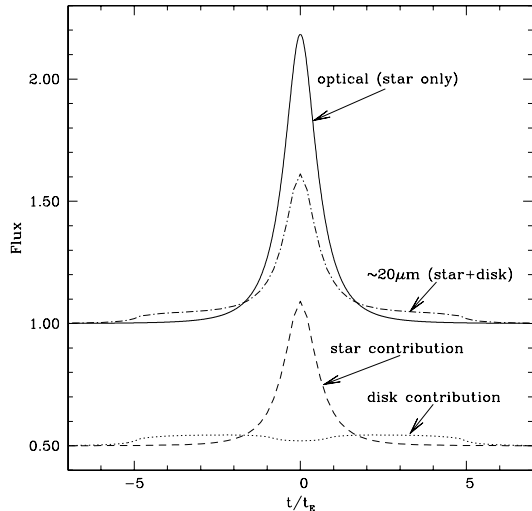


FIG. 5.— Contributions of star and disk to the lensing signal. The plot assumes that the star and the disk have the same unlensed flux at  $\sim 20\mu\text{m}$ . The dot-dashed curve shows the total lensed flux at  $\sim 20\mu\text{m}$ , which is the sum of that from the star (dashed curve) and that from the disk (dotted curve). The solid curve is the lensed flux in optical where only the star is visible. The lensing of the star+disk system is apparently chromatic because the system has different spatial structures in optical and in mid-infrared.

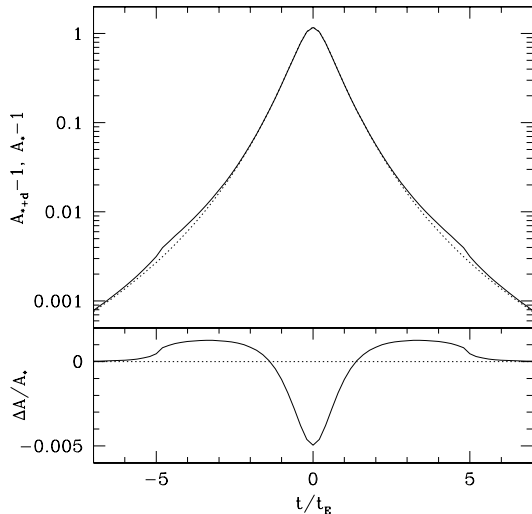


FIG. 6.— The top panel shows the classical microlensing light curve of a point source (dotted curve) and that of a star plus the disk in reflected light (solid curve). A fraction of  $\tau = 10^{-2}$  of the star light is assumed to be reflected by the disk. The bottom panel shows the relative flux difference:  $\tau(A_d/A_* - 1)$ . Parameters of the disk are the same as those used for the solid curve in panel (a) of Fig. 3.

speaking, the star-only case we mentioned before is not exactly so). The reflected light has similar spectral energy distribution as that of the star, but follows the spatial distribution of the dust in the disk. Therefore, the observed light curve carries the signature of the lensed disk at a small level. Such a light curve is illustrated in the top panel of Figure 6. The dashed curve shows the classical microlensing light curve of a point source (the star) and the solid curve shows light curve of the

star+disk system, where a fraction of  $\tau = 10^{-2}$  of the star’s light is seen in the disk. The light curve shown in Figure 5 can be thought as an extreme version of Figure 6 with  $\tau \sim 1$ . The bottom panel of Figure 6 shows the relative difference in the magnifications of the star+disk system and the star alone, i.e., the quantity  $\tau(A_d/A_* - 1)$ . It is essentially at the level of  $\tau \times 10\%$  near the wings and  $\tau \times 100\%$  near the center of the light curve. The corresponding curve follows similar parameter dependences as the ones presented in Figure 4 and can be used in the same way to constrain disk properties.

## 5. OBSERVATIONAL PROSPECTS

### 5.1. Detectability

In this section we discuss observational requirements for the detection of microlensing of circumstellar disks. As the ranges of temperature, surface brightness, and distance of the systems can be quite large, we will only provide some order of magnitude estimates for our fiducial circumstellar disk located at 8 kpc from us (see Fig.1) and for a  $1M_\odot$  lens located halfway to the Galactic center. Below we will address the detectability of the microlensing effects and will consider as an example the current specifications of the upcoming James Webb Space Telescope (JWST), which is a 6-meter telescope giving access to a wavelength range of 0.6 to  $25.5\mu\text{m}$ .

At the Galactic center, a circumstellar disk with radius as large as 100 AU has an apparent size of about  $0.01''$ , which is much smaller than the size of the telescope point spread function (PSF). As we have discussed, the properties of the disk can be probed with microlensing in several ways: from its thermal emission (peaking around  $50\mu\text{m}$ ) and from the reflected light of the star (peaking around  $1\mu\text{m}$ ). We will investigate these two possibilities separately.

The JWST cameras allow to observe in the 0.6- $25.5\mu\text{m}$  range. Between 10 and  $25\mu\text{m}$ , the main noise contributions for observing distant circumstellar disks originate from the detector self-emission and the zodiacal light (both are more important than the noise level of the star). As these two contributions scale linearly with the exposure time  $t_{\text{exp}}$ , the detection signal-to-noise ratio (S/N) of the disk is therefore proportional to  $\sqrt{t_{\text{exp}}}$ . In this wavelength range, it should be noted that the sensitivity of the detector decreases exponentially as a function of wavelength. Because of this dramatic change, systems with warmer disks peaking at shorter wavelengths will be much easier to observe.

Using the sensitivity and noise contributions given by the JWST Exposure Time Calculator for the Mid Infrared Instrument (MIRI) we have estimated several quantities: (i) The exposure time required to detect the presence of the disk, i.e., to obtain a  $3\sigma$  detection of the infrared excess at 15 and  $25.5\mu\text{m}$ , respectively. This is shown in the bottom panel of Figure 7 (gray lines) as a function of the disk-to-star luminosity ratio  $\tau$ . (ii) The exposure time required to have a  $3\sigma$  detection of a 10% change in the disk flux, i.e., to detect the microlensing signal. This is shown in solid black lines. For  $10^{-3} < \tau < 10^{-2}$ , the exposure time ranges between 1 and 100 hours. At  $10\mu\text{m}$  and below, the intensity of the blackbody spectrum of the disk decreases rapidly and does not allow any detection within a reasonable exposure time. Finally, we also point out that the current

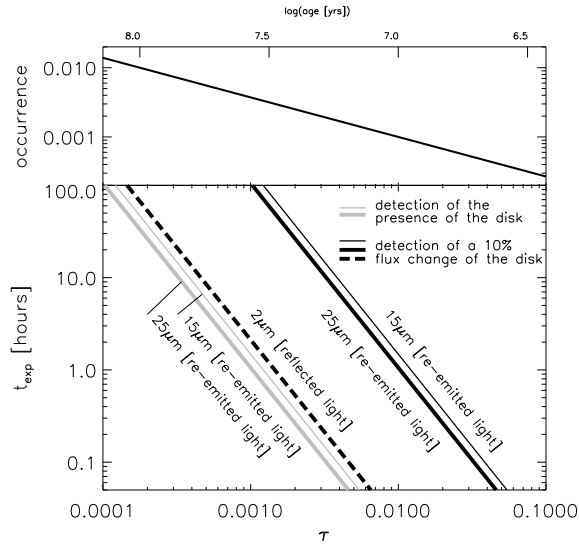


FIG. 7.— The top panel shows, as a function of the disk-to-star luminosity ratio  $\tau$ , the quantity  $\text{age}/10^{10}\text{yr}$ , corresponding to a rough estimate of the occurrence of microlensing events of circumstellar disk systems. The bottom panel presents the required exposure time to detect the disk (gray lines) and to detect a 10% change in the disk flux (solid black lines) at the  $3\sigma$  level with the JWST. The thin and thick solid lines are computed for re-emitted light at 15 and  $25.5\ \mu\text{m}$  respectively and include noise contributions from the instrument self-emission and the zodiacal light. The dashed line corresponds to the microlensing signal seen from the reflected light of the disk at  $2\ \mu\text{m}$ , for which the main source of noise comes from the star light.

observational limitations come from instrumental noise. One of the main noise contributions of MIRI is the instrument’s thermal emission. Contrary to the sensitivity in optical bands, that of mid/far-infrared detectors is expected to keep improving over the years as a result of the development of new technologies. Next generation mid-infrared detectors might therefore need significantly less exposure time than the ones quoted above and may even allow us to observe at longer wavelength where the emission from disk dominates over that of the star.

The second way for using microlensing to extract information about the disk is to measure the light reflected by the disk. In such a case, the signal is the slight deviation of the microlensing light curve from that of a point source, which is typically at the  $\tau \times 10\%$  level. We assume that the observation is performed in the K band ( $2.2\ \mu\text{m}$ ) to minimize the effect of the Galactic extinction. At this wavelength, the width of the JWST PSF is about  $0.1''$ . A rough estimate based on the Galactic stellar disk profile in Zheng et al. (2001) shows that, toward the Galactic center, the probability that another disk star falls within the PSF is less than 0.2%. Inclusion of bulge stars would increase the probability by roughly an order of magnitude. Therefore, in the case of the lensing of the circumstellar disk in reflected light observed by JWST-like space telescopes, the main contribution to the noise originates from the light of the central star (neglecting instrumental and calibration uncertainties). The dashed line in Figure 7 shows the exposure time required to have a  $3\sigma$  detection of a 10% change (caused by microlensing) in the flux of the reflected light. For  $10^{-3} < \tau < 10^{-2}$ , the exposure time ranges between  $2 \times 10^{-2}$  and 2 hours.

The duration of the microlensing event for a circumstellar disk is of the order of a year. Over such a time scale, a few exposures would allow us to sample the disk light curve with enough accuracy to constrain a number of parameters of the disk like its inner and outer radii. We note that the numbers used in this estimate are based on a typical circumstellar disk surface brightness. Brighter disks occur and would therefore reduce the exposure time mentioned above. Moreover we have based our estimates on a uniform disk. A steeper surface brightness profile will have a similar effect as reducing the effective size of the disk and therefore increase the amplitude of the magnification.

## 5.2. Event Occurrence

The disk-to-star luminosity ratio  $\tau$  of the circumstellar disk is expected to decrease as a function of the age of the system. Observationally, it has been shown that  $\tau \propto \text{age}^{-1.75}$  (Zuckerman & Song 2004). The top axis of Figure 7 labels the age of a system corresponding to the value of  $\tau$  on the bottom axis. We see that the bright phase of the circumstellar disk typically lasts for a few to  $\sim 100$  Myr, therefore the fraction of stars that have bright circumstellar disks is determined by the fraction of young stars, which is closely related to the star formation history.

For a constant star formation rate over 10 Gyr, the fraction of young stars is given by the ratio of the stars’ age and 10 Gyr. this fraction can be regarded as an order of magnitude estimate of the fraction of microlensing events that could be those of star+disk system, i.e., the occurrence of microlensing events of circumstellar disk. This is shown in the top panel of Figure 7. The values are only indicative since the star formation history of the Milky Way is much more complex than a pure continuous star formation. In the disk, there seems to be 5 episodes of enhanced star formation over the last 2 Gyr that could be related to density waves and/or perigalactic passages of satellite galaxies (de La Fuente Marcos & de La Fuente Marcos 2004). Most young stars stay near the plane where they were born since they do not have enough time to diffuse away. Therefore, along lines of sight in the Galactic mid-plane away from the bulge, the young star fraction is expected to be much higher than that shown in the top panel of Figure 7. The inner part of the Galaxy is thought to be dominated by old bulge stars. This may be true in the outer bulge. However,  $\text{H}_2$  clouds and star forming regions are present (Bania 1977; Liszt & Burton 1978) in the Galactic center. In the central few hundred parsecs of the Galaxy, there are several lines of evidence showing recent (e.g., 200 Myr ago) and ongoing star formation (see van Loon et al. 2003 and references therein). So we also expect a larger occurrence rate of systems with circumstellar disks for lines of sight toward the very center of the Galaxy. Taking these recent star formation histories into account could increase the plotted occurrence in Figure 7 by approximately an order of magnitude. A more detailed study is necessary for an accurate determination of the fraction of young stars along different lines of sight.

Presently several thousands of microlensing events have been detected toward the Galactic bulge by OGLE (e.g., Udalski et al. 2000; Wozniak et al. 2001;

Sumi et al. 2005), MOA (e.g., Sumi et al. 2003), MA-CHO (e.g., Thomas et al. 2004), and EROS (e.g., Afonso et al. 2003b). MOA<sup>2</sup>, OGLE-III<sup>3</sup> (Udalski 2003), and future experiment will provide us with a large amount of data to select candidate events of microlensing of circumstellar disks to be followed up in near- and mid-infrared. The fields monitored by current microlensing projects are along the lines of sight of low extinction regions (e.g., Baade’s window), which are typically a few degrees away from the Galactic center. To enhance the fraction of microlensing events of young stars, surveys toward the very center of the Galaxy are desired because both the Galactic center and the mid-plane of the disk are expected to have higher fraction of young stars. To minimize the extinction, such surveys needs to be done in the K band, as advocated by Gould (1995). In addition to the fraction of young stars, the microlensing optical depths is also enhanced in these surveys. For example, the microlensing optical depth of the Galactic disk is about 3 times larger toward the Galactic center than toward Baade’s window (Gould 1995). With the improvements of infrared detectors (such as mosaics of infrared arrays, e.g., Finger & Beletic 2003; Dorn et al. 2004; McLean 2004), ground-based infrared monitoring programs toward the very center of the Galaxy will become possible in the near future. Space-based infrared monitoring programs might also start in a near future with for example the Microlensing Planet Finder (MPF, see Bennett et al. 2004). They will greatly improve the search for microlensing of circumstellar disks.

Given the different timescales involved in the star and disk lensing, it is possible to observe the magnification of the disk several months or even a year after the optical microlensing event of the star. In order to optimize the use of telescope time, the following observational strategy should be followed: (i) detecting a microlensing event in the optical or infrared; (ii) if the star is likely to reside in a star-forming region or an H<sub>2</sub> cloud that indicates a young age, then following up in the near-infrared (mid-infrared) in order to detect the presences of a circumstellar disk in reflected (re-emitted) light; (iii) if a disk is present, then performing longer exposures to sparsely (e.g., once a month) sample the light curve and obtaining constraints on the disk properties. In these three steps, the second one is crucial. We want the rate of successful selection to be as high as possible. For this purpose, we can check the (projected) location of the source star to see whether it coincides with that of an H<sub>2</sub> clouds. We can also check the infrared color-magnitude diagram of neighbor stars of the source star to see whether there is any hint of young stars (e.g., the existence of evolved massive stars). (iv) In addition, one can increase the probability of observing a microlensing event of a disk by preselecting events caused by massive and nearby lenses (e.g., by choosing long duration microlensing events) in order to have larger projected Einstein ring radii and hence higher disk magnifications.

## 6. SUMMARY AND DISCUSSION

We have investigated the microlensing effects on a source star surrounded by a circumstellar disk, as a func-

tion of wavelength:

- In the mid- and far-infrared, where the emission of the system is dominated by the cold dusty disk, the microlensing light curve encodes the geometry and surface brightness profile of the disk. For a system located at the Galactic center, typical disk magnifications reach  $\sim 1.1 - 1.2$  and the events last over  $\sim 1$  year, i.e., much longer than that of the star-only case.
- At around  $20\mu\text{m}$ , where the emission for the star and the disk are in general comparable, the difference in the emission areas results in a chromatic microlensing event.
- Finally, in the near-infrared and visible, where the emission of the star dominates, the small fraction of star light directly reflected by the disk causes the light curve of the system to slightly deviate from that of a point source. In this case, typical departures from the classical microlensing light curve of a point source are at a level of  $\tau \times 10\%$ , where  $\tau$  is the disk-to-star luminosity ratio. For young disks, a photometric accuracy of  $10^{-3}$  will allow us to probe the disk properties.

We have shown how the disk light curves depend on a number of disk parameters like the size, the orientation, the inclination, the radius of the inner hole, etc., and have pointed out that in some configurations the magnification can be substantially higher. The most favorable case is the lensing of a small, highly inclined disk with a steep surface brightness profile.

Among the detected microlensing events, there is a significant fraction of events with binary lens (e.g., Alcock et al. 2000; Jaroszyński 2002; Jaroszyński et al. 2004). In the case of a binary lens, if the separation of the binary is much smaller than the circumstellar disk, the light curve would largely remain the same as that of a single lens. In addition it will better resolve the fine features of the disk such as gaps and hot spots, if they happen to come close to the caustics of the binary lens.

The duality between the infrared and optical regimes and the long timescale relevant for the disk microlensing allow us to maximize the observation efficiency by only following up systems that have already experienced a substantial magnification in the optical. The fraction of stars exhibiting a bright circumstellar disk that can be detected through the lensing effect is expected to be of order a few times  $10^{-3}$  with large variations among different lines of sight. A K band micro-lensing survey toward the very center of the Galaxy is desired for enhancements in both microlensing optical depth and occurrence rate of lensing events of circumstellar disks.

We have investigated the detectability of such events with the upcoming JWST telescope. For young disks, a few hours of exposure every month would allow us to sample the microlensing light curve of the disk and extract some disk parameters. In addition, the relatively deep exposure of the fields resulting from these observations can be used, as a byproduct, for various studies of objects toward the Galactic center.

Microlensing enables us to extend the observation of circumstellar disks to a distance far beyond the solar

<sup>2</sup> <http://www.massey.ac.nz/~iabond/alert/alert.html>

<sup>3</sup> <http://www.astro.uw.edu.pl/~ogle/ogle3/ews/ews.html>

neighborhood, in regions of different environments and metallicities. It has the potential to reveal the diversity of circumstellar disks. Studying the amount and nature of their dust and their dependence on the environment would improve our understanding of the formation and evolution of the circumstellar disks and planets.

We thank Scott Gaudi, Andy Gould, and Bohdan Paczyński for stimulating discussions and useful sugges-

tions. We are also grateful to Roman Rafikov, Dejan Vinkovic, Doron Chelouche, James Gunn, and John Bahcall for helpful discussions and comments. Z.Z. acknowledges the support of NASA through Hubble Fellowship grant HF-01181.01-A awarded by the Space Telescope Science Institute, which is operated by the Association of Universities for Research in Astronomy, Inc., for NASA, under contract NAS 5-26555. B.M. acknowledges the Florence Gould foundation for its financial support.

## REFERENCES

- Abe, F., et al. 2004, *Science*, 305, 1264  
 Afonso, C., et al. 2000, *ApJ*, 532, 340  
 Afonso, C., et al. 2003, *A&A*, 400, 951  
 Afonso, C., et al. 2003, *A&A*, 404, 145  
 Agol, E. 2003, *ApJ*, 594, 449  
 Albrow, M. D., et al. 2000, *ApJ*, 534, 894  
 Albrow, M. D., et al. 2001a, *ApJ*, 549, 759  
 Albrow, M., et al. 2001b, *ApJ*, 550, L173  
 Albrow, M. D., et al. 2001c, *ApJ*, 556, L113  
 Alcock, C., et al. 1993, *Nature*, 365, 621  
 Alcock, C., et al. 1996, *ApJ*, 461, 84  
 Alcock, C., et al. 2000, *ApJ*, 541, 270  
 Alcock, C., et al. 2000, *ApJ*, 541, 734  
 Alcock, C., et al. 2000, *ApJ*, 542, 281  
 An, J. H., et al. 2002, *ApJ*, 572, 521  
 Aubourg, E., et al. 1993, *Nature*, 365, 623  
 Bania, T. M. 1977, *ApJ*, 216, 381  
 Bennett, D. P. et al. 2004, *Proceedings of the SPIE Astronomical Telescopes and Instrumentation Symposium*, 5487, 1453  
 Bond, I. A., et al. 2004, *ApJ*, 606, L155  
 Bozza, V., & Mancini, L. 2002, *A&A*, 394, L47  
 Bozza, V., Jetzer, P., Mancini, L., & Scarpetta, G. 2002, *A&A*, 382, 6  
 Calchi Novati, C., et al. 2005, *A&A*, submitted (astro-ph/0504188)  
 Cassan, A., et al. 2004, *A&A*, 419, L1  
 Castro, S., Pogge, R. W., Rich, R. M., DePoy, D. L., & Gould, A. 2001, *ApJ*, 548, L197  
 de La Fuente Marcos, R., & de La Fuente Marcos, C. 2004, *New Astronomy*, 9, 475  
 Dorn, R. J., Finger, G., Huster, G., Lizon, J. L., Mehrgan, H., Meyer, M., Steigmeier, J., & Moorwood, A. F. M. 2004, *Scientific Detectors for Astronomy, The Beginning of a New Era*, 523  
 Fields, D., et al. 2003, *ApJ*, 596, 1305  
 Finger, G., & Beletic, J. W. 2003, *Proc. SPIE*, 4841, 839  
 Gaudi, B. S., & Gould, A. 1999, *ApJ*, 513, 619  
 Gaudi, B. S., et al. 2002, *ApJ*, 566, 463  
 Ghosh, H., et al. 2004, *ApJ*, 615, 450  
 Gould, A. 1992, *ApJ*, 392, 442  
 Gould, A. 1994, *ApJ*, 421, L71  
 Gould, A. 1995, *ApJ*, 446, L71  
 Gould, A., & Loeb, A. 1992, *ApJ*, 396, 104  
 Gould, A. 2001, *PASP*, 113, 903  
 Gould, A., Bennett, D. P., & Alves, D. R. 2004, *ApJ*, 614, 404  
 Hendry, M. A., Coleman, I. J., Gray, N., Newsam, A. M., & Simmons, J. F. L. 1998, *New Astronomy Review*, 42, 125  
 Heyrovsky, D., & Loeb, A. 1997, *ApJ*, 490, 38  
 Jaroszyński, M. 2002, *Acta Astronomica*, 52, 39  
 Jaroszyński, M., et al. 2004, *Acta Astronomica*, 54, 103  
 Jiang, G., et al. 2004, *ApJ*, 617, 1307  
 Koerner, D. W., Sargent, A. I., & Ostroff, N. A. 2001, *ApJ*, 560, L181  
 Kubas, D., et al. 2005, *A&A*, 435, 941  
 Kuchner, M. J., & Holman, M. J. 2003, *ApJ*, 588, 1110  
 Liszt, H. S., & Burton, W. B. 1978, *ApJ*, 226, 790  
 Mao, S., & Paczyński, B. 1991, *ApJ*, 374, L37  
 McLean, I. S. 2004, *Scientific Detectors for Astronomy, The Beginning of a New Era*, 1  
 Moran, S. M., Kuchner, M. J., & Holman, M. J. 2004, *ApJ*, 612, 1163  
 Natta, A., Prusti, T., Neri, R., Wooden, D., Grinin, V. P., & Mannings, V. 2001, *A&A*, 371, 186  
 Paardekoooper, S.-J., & Mellema, G. 2004, *A&A*, 425, L9  
 Paczyński, B. 1986, *ApJ*, 304, 1  
 Papaloizou, J., & Lin, D. N. C. 1984, *ApJ*, 285, 818  
 Popowski, P., et al. 2003, In "Gravitational Lensing: A Unique Tool For Cosmology", Aussois 2003, eds. D. Valls-Gabaud & J.-P. Kneib, astro-ph/0304464  
 Quillen, A. C., & Thorndike, S. 2002, *ApJ*, 578, L149  
 Sasselov, D. 1997, In "Variables Stars and the Astrophysical Returns of the Microlensing Surveys", eds. Roger Ferlet, Jean-Pierre Maillard & Brigitte Raban, p141  
 Sumi, T., et al. 2003, *ApJ*, 591, 204  
 Sumi, T., et al. 2005, *ApJ*, submitted, ArXiv Astrophysics e-prints, arXiv:astro-ph/0502363  
 Simmons, J. F. L., Newsam, A. M., Willis, J. P. 1995, *MNRAS*, 276, 182  
 Thomas, C. L., et al. 2004, *ApJ*, submitted (astro-ph/0410341)  
 Tisserand, P., & Milsztajn, A. 2005, In the proceedings of the 5th Rencontres du Vietnam, "New Views on the Universe", Hanoi, Aug 5-11, 2004 (astro-ph/0501584)  
 Udalski, A., et al. 1993, *Acta Astron.* 43, 289  
 Udalski, A., et al. 1994, *Acta Astron.* 44, 1  
 Udalski, A., Zebrun, K., Szymanski, M., Kubiak, M., Pietrzynski, G., Soszynski, I., & Wozniak, P. 2000, *Acta Astronomica*, 50, 1  
 Udalski, A. 2003, *Acta Astronomica*, 53, 291  
 Udalski, A., et al. 2005, *ApJ*, submitted (astro-ph/0505451)  
 Valls-Gabaud, D. 1998, *MNRAS*, 294, 747  
 van Loon, J. T., et al. 2003, *MNRAS*, 338, 857  
 Wahhaj, Z., Koerner, D. W., Ressler, M. E., Werner, M. W., Backman, D. E., & Sargent, A. I. 2003, *ApJ*, 584, L27  
 Wilner, D. J., Holman, M. J., Kuchner, M. J., & Ho, P. T. P. 2002, *ApJ*, 569, L115  
 Wozniak, P. R., Udalski, A., Szymanski, M., Kubiak, M., Pietrzynski, G., Soszynski, I., & Zebrun, K. 2001, *Acta Astronomica*, 51, 175  
 Wyatt, M. C., & Dent, W. R. F. 2002, *MNRAS*, 334, 589  
 Zheng, Z., Flynn, C., Gould, A., Bahcall, J. N., & Salim, S. 2001, *ApJ*, 555, 393  
 Zuckerman, B. 2001, *ARA&A*, 39, 549  
 Zuckerman, B., & Song, I. 2004, *ApJ*, 603, 738